



T1 and T2 mapping to detect chronic inflammation in cardiac magnetic resonance imaging in heart failure with reduced ejection fraction

Tilman Emrich^{1,2*} , Felix Hahn¹ , David Fleischmann¹, Moritz C. Halfmann¹, Christoph Düber¹, Akos Varga-Szemes³, Felicitas Escher^{4,7}, Evgenia Pefani⁵, Thomas Münzel^{2,5}, Heinz-Peter Schultheiss⁴, Karl-Friedrich Kreitner¹ and Philip Wenzel^{2,5,6}

¹Department of Diagnostic and Interventional Radiology, University Medical Center Mainz, Mainz, Germany; ²German Center for Cardiovascular Research (DZHK), partner site Rhine-Main, Mainz, Germany; ³Department of Radiology and Radiological Science, Medical University of South Carolina, Charleston, SC, USA; ⁴IKDT Institut Kardiale Diagnostik und Therapie GmbH, Berlin, Germany; ⁵Center for Cardiology, Cardiology 1, University Medical Center Mainz, Mainz, Germany; ⁶Center for Thrombosis and Hemostasis, University Medical Center Mainz, Mainz, Germany; ⁷Department of Cardiology, Campus Virchow-Klinikum, Charité–University Medicine Berlin, Berlin, Germany

Abstract

Aims The purpose of this retrospective single-centre study was to evaluate the non-invasive detection of endomyocardial biopsy (EMB)-established chronic myocardial inflammation in patients with heart failure with reduced ejection fraction (HFrEF) using T1 and T2 mapping.

Methods and results The study population consisted of 52 retrospectively identified HFrEF patients who underwent EMB and cardiac magnetic resonance imaging at 3 Tesla. EMB was defined according to the position statement of the European Society of Cardiology and served as reference to identify inflammation in all patients. A control group of healthy volunteers with prior cardiac magnetic resonance imaging studies ($n = 58$) was also identified. Global and segmental T1 and T2 values as well as septal measurements and tissue heterogeneity parameters were calculated.

Out of the 52 patients with HFrEF, 33 patients had myocardial inflammation detected by EMB, while 19 patients were EMB negative for inflammation. Mean left ventricular ejection fraction was 31% in both groups ($P = 0.97$). Global T1 and T2 values in HFrEF patients were significantly higher compared with healthy controls (T1 1275 ± 69 ms vs. $1,175 \pm 44$ ms, $P < 0.001$; T2 40.0 ± 3.4 ms vs. 37.9 ± 1.6 ms, $P < 0.001$). The distribution of T1 and T2 values between patients with and without EMB-proven chronic myocardial inflammation was not statistically different when regarding global (T1 1292 ± 71 ms vs. 1266 ± 67 ms, $P = 0.26$; T2 40.0 ± 2.6 ms vs. 40.0 ± 3.9 ms, $P = 1.0$), septal (T1 1299 ± 63 ms vs. 1289 ± 76 ms, $P = 0.76$; T2 40.1 ± 3.5 ms vs. 40.0 ± 6.4 ms, $P = 0.49$) or maximum segmental values (T1 1414 ± 111 ms vs. 1363 ± 88 ms, $P = 0.15$; T2 47.3 ± 5.2 ms vs. 48.8 ± 11.8 ms, $P = 0.53$). Mean absolute deviation of segmental T1 and T2 values and log-transformed pixel-wise standard deviation as parameters of tissue heterogeneity did not reveal statistical significant differences between inflammation-positive and inflammation-negative HFrEF patients (all $P > 0.4$).

Conclusions Conventionally performed quantitative T1 and T2 mapping values significantly correlated with prevalence of HFrEF but did not discriminate HFrEF patients with or without chronic myocardial inflammation in our cohort. This suggests that EMB is the preferred method to detect chronic myocardial inflammation in HFrEF.

Keywords HFrEF; DCM phenotype; CMR; Mapping; Inflammation

Received: 4 February 2020; Revised: 20 April 2020; Accepted: 23 May 2020

*Correspondence to: Tilman Emrich, Department of Diagnostic and Interventional Radiology, University Medical Center Mainz, Langenbeckstr. 1, 55131 Mainz, Germany. Tel: +49 6131 17 5825; Fax: +49 6131 17 6333. Email: tilman.emrich@unimedizin-mainz.de
Tilman Emrich and Felix Hahn contributed equally to this work.

Introduction

Cardiovascular disease is responsible for approximately 30% of deaths worldwide. While the majority of cardiovascular disease deaths are attributable to ischaemic heart disease, non-ischaemic, non-valvular heart failure still represents a significant cause of morbidity and mortality.^{1,2} In patients with non-ischaemic heart failure with reduced ejection fraction (HFrEF), dilation and impaired contraction of the left or both ventricles lead to mainly systolic and/or diastolic (bi) ventricular dysfunction, called dilated cardiomyopathy (DCM).³ Among patients with non-ischaemic non valvular heart failure, DCM-like phenotype represents the most common type of cardiomyopathy with an estimated incidence of 1 in 250 adults.^{4,5}

The aetiologies resulting in a DCM phenotype are manifold.⁶ However, myocardial inflammation can often be observed in HFrEF and may represent a precursor, concomitant factor (i.e. epiphenomenon) or driver of DCM.^{7,8} Detection of inflammation may also trigger disease-specific therapeutic approaches in viral myocarditis and certain forms of autoimmune disease (e.g. Churg Strauss vasculitis or giant cell myocarditis). In selected cases, unspecific immunosuppression with azathioprine and prednisolone may be initiated in addition to pharmacotherapy, which has been shown to improve left ventricular (LV) function and prognosis in chronic HFrEF patients with virus-negative inflammation.⁹

In the diagnostic pathway of HFrEF patients, endomyocardial biopsy (EMB) enables physicians to detect or rule out myocardial inflammation, interstitial fibrosis, and presence of viral genome. According to current consensus statements, EMB should be performed in the early course of the disease, in particular in individuals with haemodynamic compromise or heart rhythm disorders, or who are refractory to medical therapy. To minimize sampling errors and increase diagnostic accuracy, current guidelines propose that at least three samples should be taken.¹⁰ While EMB is an invasive procedure, the complication rate of right or LV EMB is considered to be low.^{11,12}

Myocardial T1 and T2 mapping techniques in cardiac magnetic resonance (CMR) imaging have recently shifted the focus from qualitative to quantitative analysis of the myocardial tissue.^{13–15} There is potential that mapping values or ranges thereof have the discriminatory ability to help detect subtypes of cardiomyopathies or identify patients at risk. However, the widespread use of mapping techniques is currently still hindered by the limitation that T1 and T2 values are challenging to standardize.¹⁶

A major challenge of CMR in chronic heart failure patients is to differentiate between patients with inflammation versus those without inflammation, which is probably the most difficult scenario to face. In a recent study by Spieker *et al.*, a T2 cut-off value has been proposed that may help to identify patients with myocardial inflammation who would

benefit from EMB.¹⁷ Because the presence of inflammation in HFrEF patients may change treatment protocol,^{2,10} the possibility to non-invasively and reliably detect myocardial inflammation has major clinical relevance.

Therefore, the aim of this study was to retrospectively validate the non-invasive detection of immunohistochemically established myocardial inflammation using T1 and T2 mapping in a cohort of stable, chronic HFrEF patients.

Methods

Study population

A total of 157 patients were retrospectively identified who had undergone EMB and invasive coronary angiography at our tertiary referral centre between November 2015 and October 2017 according to current guideline recommendations.¹⁸ Out of the 157 patients, 57 were found who had also undergone CMR imaging within a median delay of 2 days relative to the EMB, which showed LV or biventricular systolic dysfunction and dilatation in the absence of valvular or coronary heart disease ('DCM-like' phenotypes). Five patients were excluded due to severe motion artefacts and arrhythmias; the remaining 52 patients were included in this study. In addition, a group of 58 healthy volunteers that had been previously investigated to establish reference mapping values for our centre served as a control group. The study was approved by the local ethics committee with a waiver for informed consent (837.196.13/837.477.14).

Cardiac magnetic resonance imaging and post-processing

CMR was performed using a 3.0 T scanner (MAGNETOM Prisma, Siemens, Erlangen, Germany) with an 18-channel body coil. The CMR protocol involved the following acquisitions: (i) cine sequences including horizontal long axis (HLA) and a stack of short axis (SAX) covering the LV; (b) native T1 mapping in two HLA and three SAX (base, midventricular, and apex); (c) native T2 mapping in two HLA and three SAX (base, midventricular, and apex); and (d) phase-sensitive inversion-recovery images in HLA and SAX orientation covering the LV for assessment of late gadolinium enhancement after contrast administration (0.2 mmol/kg gadoteric acid). For T1 mapping, a commercially available modified Look Locker inversion-recovery (MOLLI) sequence with a 5(3)3-scheme was used with TR 280.56 ms, TE 1.12 ms, FOV 360 mm, slice thickness 8 mm, and flip angle 35°. For T2 mapping, a T2 preparation sequence with three preparation pulses of duration 0.0, 30.0, and 55.0 ms and a recovery period of 3 heart beats was used applying the following parameters: TR

207.39 ms, TE 1.32 ms, FOV 360 mm, slice thickness 8 mm, and flip angle 12°. For the purpose of this study, T1 and T2 maps were analysed.

T1 and T2 maps were calculated using a third-party dedicated cardiovascular software (CVI 42 v5.9.3, Circle Cardiovascular Imaging Inc., Calgary, Canada). Segmentation was performed according to the American Heart Association 17-segment model,¹⁹ and segments with severe artefacts were excluded from further analyses. To avoid inclusion of blood or epicardial fat, the inner and outer 25% of the 'donut' myocardial regions of interest were discarded.

Endomyocardial biopsy and histological analysis

Selective angiograms of the left and right coronary arteries were obtained to exclude coronary artery disease. EMB was performed using a transradial arterial or femoral arterial or femoral venous access, and ventricular biopsies were taken from the septal or apical regions under fluoroscopic guidance.²⁰

Histologic and immunohistologic analyses were performed in a CAP-accredited laboratory (Institute for Cardiac

Diagnostic and Therapy Berlin, Germany, CAP No. 7182802, AU-ID:1397839), blinded to the results of CMR. Immunohistochemistry was used for the characterization of inflammatory infiltrates.¹⁰ For immunohistological evaluation, specimens were embedded in Tissue Tec (SLEE, Mainz, Germany) and immediately snap frozen in methyl butane that had been cooled in liquid nitrogen and then stored at -80°C until processing. Embedded specimens were cut serially into cryosections of 5 mm thickness and placed on 10% poly-L-lysine-pre-coated slides. Myocardial inflammation was diagnosed by 14.0 lymphocytes/ mm^2 with the presence of >7.0 CD3 + lymphocytes/ mm^2 according to the European Society of Cardiology position statement.⁸ Furthermore, presence of macrophages (threshold > 35.0 CD11b+/Mac-1 + macrophages/ mm^2) and perforin-positive cytotoxic cells (threshold > 2.9 cells/ mm^2) was diagnostic of myocardial inflammation.²¹ Antibodies used: CD3 + lymphocytes (Dako, Glostrup, Denmark, dilution 1:25), CD11a+/LFA-1 + lymphocytes (Immuno Tools, Friesoythe, Germany, dilution 1:250), and CD11b+/Mac-1 + macrophages (ImmunoTools, dilution 1:500). Perforin-positive cellular infiltrates were also defined by immunohistochemistry (clone δG9 , BD Bioscience, San Jose, CA, USA, dilution 1:150). The staining and

Table 1 Baseline characteristics of the study population

		Controls (<i>n</i> = 58)	EMB– HFrEF (<i>n</i> = 19)	EMB+ HFrEF (<i>n</i> = 33)	<i>P</i> value ^a
Age, years		50 ± 15	54 ± 18	53 ± 14	0.85
Sex, <i>n</i> (%)	Male	32 (55)	14 (74)	23 (70)	1.0
	Female	26 (45)	5 (26)	10 (30)	
BMI, kg/m^2		24.1 ± 4.1	27.4 ± 6.6	27.8 ± 5.6	0.67
Symptoms, <i>n</i> (%)	Dyspnoea	0	15 (79)	25 (76)	1.0
	Palpitations	0	8 (42)	6 (18)	0.10
	NYHA I II	0	12 (63)	23 (70)	0.76
	NYHA III IV	0	7 (37)	10 (30)	
	Decompensation	0	11 (58)	22 (67)	0.56
Onset of Symptoms, <i>n</i> (%)	<2 weeks	0	5	14	0.35
	2 weeks–3 months	0	8	8	
	>3 months	0	6	11	
Heart rhythm disorders, <i>n</i> (%)	Ventricular arrhythmias	0	1 (5)	2 (6)	1.0
	Bundle branch block	0	11 (58)	12 (36)	0.16
Left ventricular ejection fraction, %		60 ± 6	31 ± 13	31 ± 12	0.97
NT-proBNP, pg/mL, median [IQR]		n/a	300 [151–967]	409 [106–1,083]	0.90
EMB results	Lymphocyte count/ mm^2 , median [IQR]	n/a	9 [3–11]	27 [18–40]	<0.001
	CD3 + cell count/ mm^2 , median [IQR]	n/a	1 [0–3]	15 [8–30]	<0.001
	MAC1 + cell count/ mm^2 , median [IQR]	n/a	16 [9–22]	48 [36–68]	<0.001
	Perforin + cell count/ mm^2 , median [IQR]	n/a	0.0 [0.0–0.0]	0.1 [0.0–2.2]	0.004
	Viral infection with active replication, <i>n</i> (%) ^b	n/a	1 (5) ^c	1 (3) ^d	1.0
	Fibrosis, <i>n</i> (%)	n/a	12 (63)	24 (73)	0.54

EMB– HFrEF, EMB negative for inflammation; EMB+ HFrEF, EMB positive for inflammation.

^aComparison between EMB– and EMB+ HFrEF patients.

^bAround 16 out of 19 of EMB– HFrEF patients (80%; viral types were erythrovirus, *n* = 12; and HHV; *n* = 6) and 26 out of 33 EMB+ HFrEF patients (81%; viral types were erythrovirus, *n* = 23; HHV, *n* = 10; and EBV, *n* = 2) showed presence of viral genome without active replication. The sum of the viruses can be more than 100% because patients could have more than one viral genome present.

^cViral type was Erythrovirus (number of copies 1195/ μg DNA).

^dViral type was Erythrovirus (number of copies 1063/ μg DNA).

peroxidase reactions in all samples were carried out identically for all samples.²² Immunoreactivity was quantified by digital image analysis.²³

Statistical analysis

Statistical analysis was performed using the statistical software package R 3.5.1.²⁴ All continuous data are given as

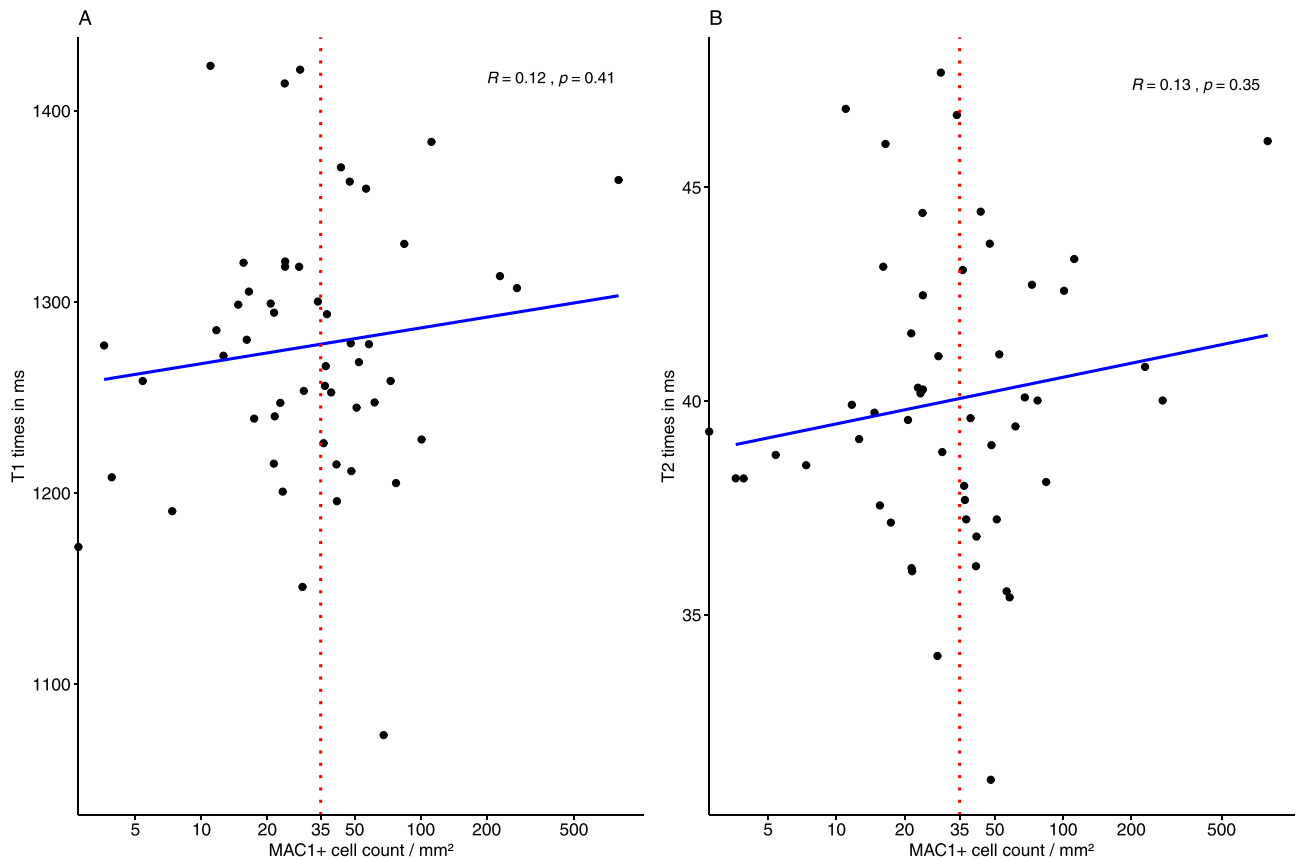
mean ± standard deviation or median with interquartile range, where appropriate. Testing for group differences was performed by using the exact Fisher test, Wilcoxon sum-rank test, or Welch independent T-test after assessing normality distribution of data. Besides comparing mean and maximum values of global, midventricular, and septal regions of interest, mean absolute deviation of segmental and log-transformed pixel-wise standard deviation were computed and evaluated as proposed previously.²⁵ Linear support

Table 2 Comparison of quantitative T1 and T2 values in the heart failure with reduced ejection fraction groups

		EMB− HFrEF (n = 19)	EMB+ HFrEF (n = 33)	P value
T1, ms	Global mean	1292 ± 71	1266 ± 67	0.26
	Midventricular mean	1280 ± 68	1258 ± 68	0.35
	Midventricular septal	1299 ± 63	1289 ± 76	0.76
	Maximum segmental	1414 ± 111	1363 ± 88	0.15
T2, ms	Global mean	40.0 ± 2.6	40.0 ± 3.9	1.00
	Midventricular mean	39.6 ± 2.4	40.0 ± 5.1	0.82
	Midventricular septal	40.1 ± 3.5	40.0 ± 6.4	0.49
	Maximum segmental	47.3 ± 5.2	48.8 ± 11.8	0.53
MAD	mean segmental T1, ms	45.3 ± 15.9	42.8 ± 18.3	0.47
	mean segmental T2, ms	2.5 ± 0.9	2.9 ± 2.0	0.68
	log-transformed pixel standard deviation T1	0.31 ± 0.07	0.29 ± 0.08	0.40
	log-transformed pixel standard deviation T2	0.27 ± 0.08	0.29 ± 0.14	0.87

EMB−, EMB negative for inflammation; EMB+, EMB positive for inflammation; MAD, mean absolute deviation.

Figure 1 Scatterplots of (A) mean T1 times and (B) mean T2 times in relation to MAC1+ cell count with regression lines depicted in blue. Red vertical line at MAC1+ cell count = 35/mm² depicting cut-off.



vector machines were fitted using the R package 'e1071' (<https://CRAN.R-project.org/package=e1071>, last accessed 30.11.2019). P values < 0.05 were considered statistically significant.

Results

Out of the 52 patients with HFrEF and DCM-like phenotype, 33 patients had myocardial inflammation detected by EMB, while 19 patients were EMB negative for inflammation. Mean LV ejection fraction was 31% in both groups. Further baseline characteristics of the patient cohort as well as the healthy control group are depicted in *Table 1*.

Mean global T1 and T2 values in HFrEF patients were significantly higher compared with healthy volunteers (T1 1275 ± 69 ms vs. 1175 ± 44 ms, $P < 0.001$; T2 40.0 ± 3.4 ms vs. 37.9 ± 1.6 ms, $P < 0.001$). However, the distribution of T1 and T2 values between patients with and without EMB-proven myocardial inflammation was not statistically different when regarding global ($P = 0.26$ and

$P = 1.0$ respectively), midventricular septal ($P = 0.76$ and $P = 0.49$, respectively), or maximum segmental values ($P = 0.15$ and $P = 0.53$, respectively, cf. *Table 2* and *Figures 1* and *2*). Mean absolute deviation of segmental T1 and T2 values and log-transformed pixel-wise standard deviation as parameters of tissue heterogeneity did not reveal statistical significant differences between inflammation-positive and inflammation-negative HFrEF patients (*Table 2*).

The distribution of T1 and T2 relaxation times is shown in *Figure 3*. While the relaxation times of healthy volunteers were more tightly clustered around their lower mean relaxation times, HFrEF patients showed a larger variance especially regarding T2 relaxation times. Correspondingly, fitting a linear support vector machine to classify healthy volunteers from patients with HFrEF resulted in 86% sensitivity (50/58) and 83% specificity (43/52), whereas fitting a linear support vector machine to classify inflammation-negative from inflammation-positive chronic HFrEF patients resulted in 88% sensitivity (29/33) and a poor 16% specificity (3/19).

An exemplary depiction of two patients with similar T1 and T2 relaxation times but different inflammation status is displayed in *Figure 4*.

Figure 2 Mean T1 and T2 times with regards to group and inflammation. HV, healthy volunteers; EMB– HFrEF DCM, HFrEF patients without inflammation in EMB; EMB+ HFrEF, HFrEF patients with inflammation in EMB.

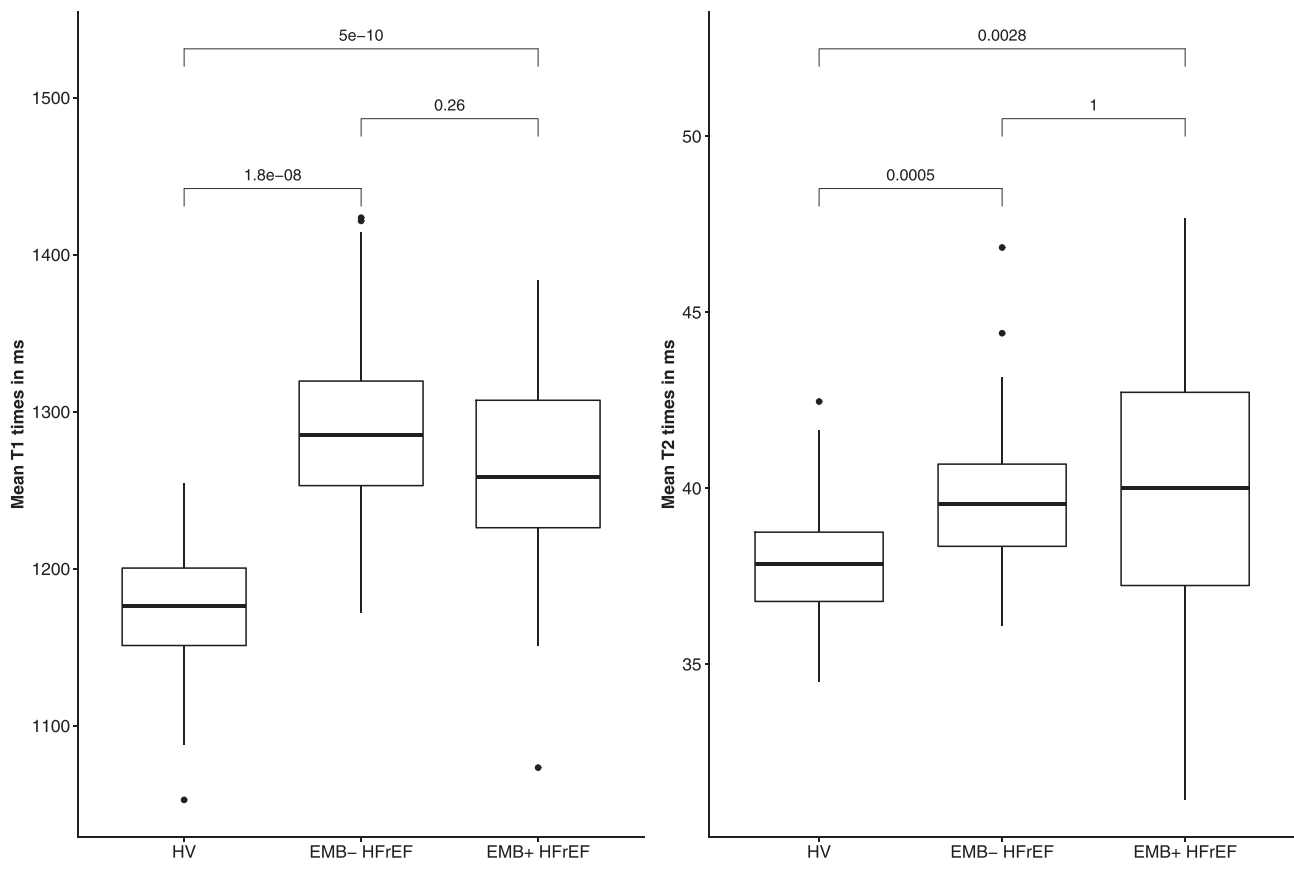
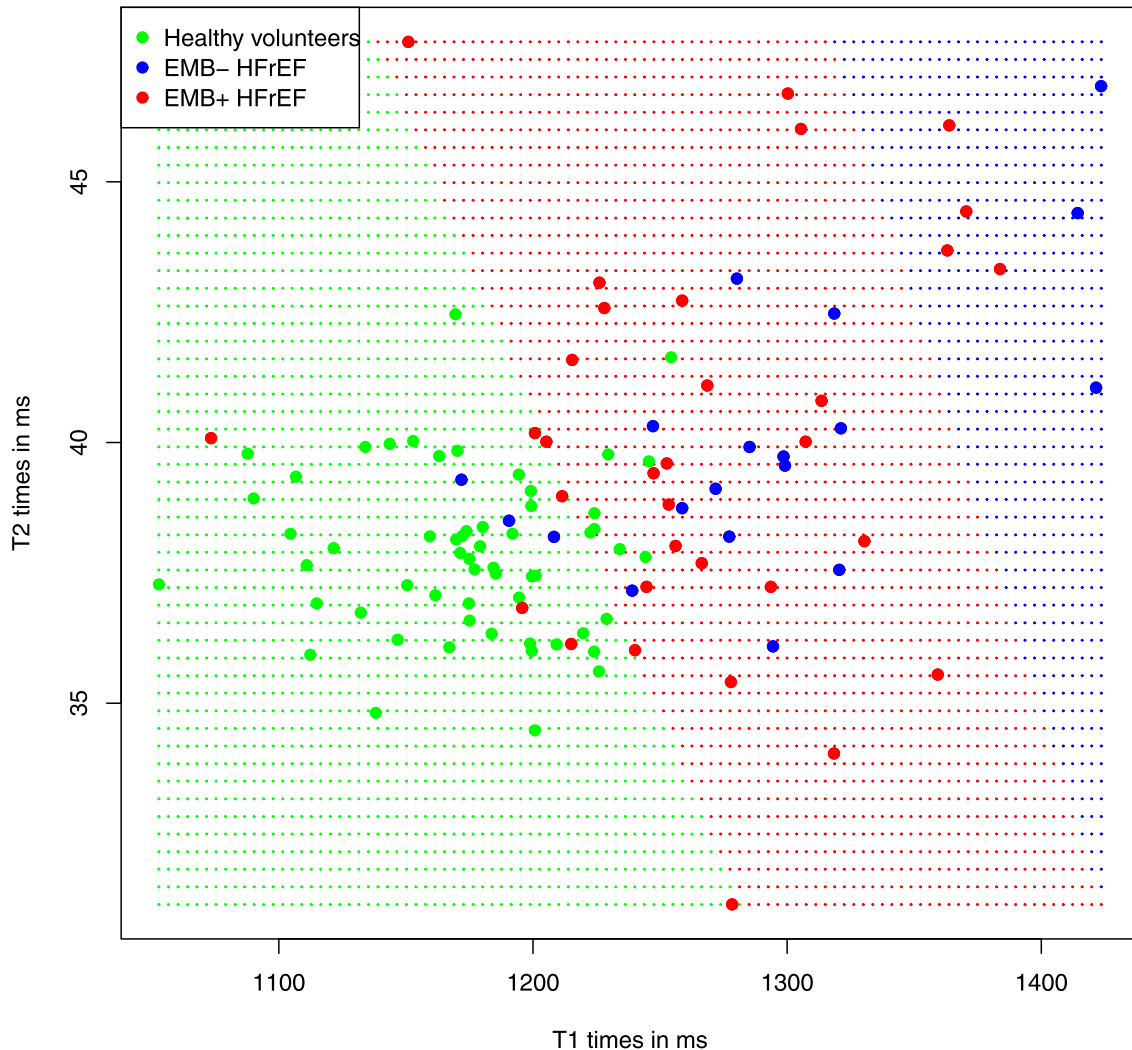


Figure 3 Linear SVM classifiers fitted to the cohort (small dotted points indicate prediction of SVMs, larger points indicate ground truth). SVM, support vector machine; EMB– HFrEF, HFrEF patients without inflammation in EMB; EMB+ HFrEF, HFrEF patients with inflammation in EMB.



Discussion

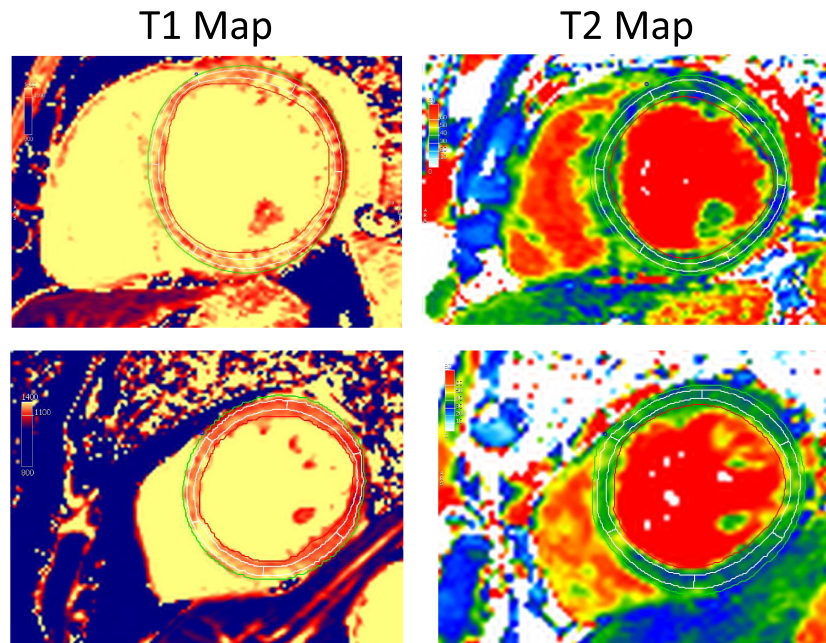
In this retrospective analysis of our monocentric cohort of HFrEF patients with DCM phenotype, both T1 and T2 mapping were robust identifiers of diseased patients compared with healthy controls. However, neither conventionally assessed global T1 and T2 mapping values nor mapping variants such as midventricular septal measurements or mean absolute deviations were able to significantly discriminate presence from absence of myocardial inflammation in patients with chronic HFrEF.

Compared with a control group of healthy volunteers, both T1 and T2 relaxation times were significantly elevated in our cohort of HFrEF patients. This is in accordance with previously published studies.^{26,27} However, literature on the performance of CMR to detect chronic inflammation in patients

with HFrEF is limited. In their cohort, Spieker *et al.* demonstrated a significant difference in the distribution of T2 times in patients with and without inflammatory cells.¹⁷ However, it is important to note that their T2 cut-off value did not help to single out patients with presence of inflammatory cells but rather was a cut-off below which patients did not show inflammatory cells in EMB.

Baessler *et al.* investigated texture analysis in a subset of magnetic resonance imaging in myocarditis (MyoRacer) trial patients (ClinicalTrials.gov registration no. NCT02177630), which consisted of patients with chronic heart failure-like myocarditis.²⁸ In their publication, the authors did not find significant differences in conventional T1 and mean T2 times in 26 patients with EMB-proven inflammation and 14 patients without EMB-proven inflammation (1066 ± 752 ms vs.

Figure 4 Exemplary figure of two patients with similar T1 and T2 relaxation times, but different inflammation status (upper row myocardial T1 time 1277 ms, T2 time 38 ms, lymphocyte count 4/mm², MAC 1 + count 4/mm²; lower row myocardial T1 time 1247 ms, T2 time 39 ms, lymphocyte count 38/mm², MAC 1 + count 52/mm²).



1066 ± 688 ms, $P = 0.83$; and 63.4 ± 5.3 ms vs. 61.1 ± 3.1 ms, $P = 0.22$, respectively). However, the size of their patient cohort was small. In an older study by Lurz *et al.* that did not use mapping techniques, the diagnostic performance of CMR in patients with suspected chronic myocarditis was not sufficient to guide clinical management as well.²⁹

There are multiple differences between the aforementioned referenced studies and our investigation that may explain the discordant outcome of the three studies. While Spieker *et al.* and Baessler *et al.* conducted CMR scans at 1.5 T, we performed the studies at 3.0 T. Furthermore, there is a variety of T1 mapping techniques, such as MOLLI, shortened MOLLI (ShMOLLI), and saturation recovery single shot acquisition, that may provide different T1 results. For T1 mapping, Baessler *et al.* used a 3(3)5 MOLLI scheme, whereas a 5(3)3 MOLLI scheme was used in our study. T2 maps are calculated using either a multiecho spin-echo or a steady-state free precession sequence.^{30,31} In the MyoRacer trial, T2 maps were only acquired at 1.5 T.³² The impact of the field strength and the chosen mapping technique on the ability to detect myocardial inflammation remains unknown. Interestingly, 1.5 T might prove more sensitive than 3.0 T for the detection of myocardial oedema and therefore be favourable for diagnosis of acute myocardial inflammation. It is also important to note that the definition of inflammation differs between the studies. While Spieker *et al.* considered the presence of >14 infiltrating leucocytes/mm² and the presence of >2 CD3-positive lymphocytes per

high-power field as diagnostic for myocardial inflammation,¹⁷ Baessler *et al.* set the cut-off value of at least 20 infiltrating immune cells per square millimetre (CD3 T-lymphocytes and/or CD68 macrophages) as diagnostic for myocardial inflammation.²⁸

In addition to quantitative analysis of mapping values, texture analysis and radiomics of T1 and T2 maps have become a focus of investigations lately across all radiological fields.^{33,34} While preliminary studies are promising, texture analysis software regularly outputs a large number of parameters, resulting in challenging data interpretation because multiple hypothesis testing has to be taken into account and reproducibility has been limited up to date.³⁵

As current guidelines state that immunosuppression may be considered after detection of virus-negative myocardial inflammation by EMB in selected cases,^{2,9} failure of CMR to reliably detect inflammation fosters the role of EMB in the work-up of chronic HFrEF and DCM patients, or the need for a combined work-up including CMR and EMB, for the time being.³⁶ Therefore, in contrast to acute phase, in patients with chronic heart failure, the diagnostic performance of CMR has to be considered as not sufficient to guide clinical management so far.

The rate of adverse events related to EMB is low and combination with coronary angiography is possible.³⁷ Position papers also postulate that follow-up EMB may be required to guide the intensity and length of immunosuppression.⁸ Therefore, future studies should evaluate the predictive

ability of quantitative mapping analyses to compare initial and follow-up CMR studies with respect to inflammatory changes in EMB.

Our study has some limitations. First and foremost, the study was single-centred and conducted in a retrospective fashion. Moreover, our final sample size was limited consisting of only 52 patients. While EMB is widely accepted as the gold standard for diagnosing myocardial inflammation, a sampling error leading to false-negative results cannot be excluded.

In conclusion, conventionally performed quantitative T1 and T2 mapping values were not able to reliably detect myocardial inflammation in chronic HFrEF patients with DCM phenotype in our cohort, thus suggesting that EMB should remain an essential part in the diagnostic work-up to test for myocardial inflammation. There is hope that further texture analysis approaches have the potential to overcome the hurdles in quantitative T1 and T2 mapping. However, while preliminary studies have been promising, reproducibility has still to be demonstrated.

Acknowledgements

TE and FH contributed equally to this work. This study contains parts of the doctoral thesis of one of the authors (DF).

Conflict of interest

TE has received a speaker fee and travel support from Siemens Healthineers, AVS receives institutional research support and travel support from Siemens Healthineers and is consultant for Elucid Bioimaging. None of these companies supported this study, and none of the authors reports a conflict of interest.

Funding

PW is supported by a grant from the Bundesministerium für Bildung, Wissenschaft, Forschung und Technologie (BMBF 01EO1503). TM and PW are Principal Investigators of the German Centre of Cardiovascular Research (DZHK).

References

- Roth GA, Huffman MD, Moran AE, Feigin V, Mensah GA, Naghavi M, Murray CJL. Global and regional patterns in cardiovascular mortality from 1990 to 2013. *Circulation* 2015; **132**: 1667–1678.
- Pinto YM, Elliott PM, Arbustini E, Adler Y, Anastakis A, Böhm M, Duboc D, Gimeno J, de Groote P, Imazio M, Heymans S, Klingel K, Komajda M, Limongelli G, Linhart A, Mogensen J, Moon J, Pieper PG, Seferovic PM, SchueWwler S, Zamorano JL, Caforio ALP, Charron P. Proposal for a revised definition of dilated cardiomyopathy, hypokinetic non-dilated cardiomyopathy, and its implications for clinical practice: a position statement of the ESC working group on myocardial and pericardial diseases. *Eur Heart J* 2016; **37**: 1850–1858.
- Jefferies JL, Towbin JA. Dilated cardiomyopathy. *Lancet* 2010; **375**: 752–762.
- McKenna WJ, Maron BJ, Thiene G. Classification, epidemiology, and global burden of cardiomyopathies. *Circ Res* 2017; **121**: 722–730.
- Codd MB, Sugrue DD, Gersh BJ, Melton LJ. Epidemiology of idiopathic dilated and hypertrophic cardiomyopathy. A population-based study in Olmsted County, Minnesota, 1975–1984. *Circulation* 1989; **80**: 564–572.
- Hershberger RE, Hedges DJ, Morales A. Dilated cardiomyopathy: the complexity of a diverse genetic architecture. *Nat Rev Cardiol* 2013; **10**: 531–547.
- Kawai C. From myocarditis to cardiomyopathy: mechanisms of inflammation and cell death: learning from the past for the future. *Circulation* 1999; **99**: 1091–1100.
- Caforio ALP, Pankuweit S, Arbustini E, Basso C, Gimeno-Blanes J, Felix SB, Fu M, Heliö T, Heymans S, Jahns R, Klingel K, Linhart A, Maisch B, McKenna W, Mogensen J, Pinto YM, Ristic A, Schultheiss H-P, Seggewiss H, Tavazzi L, Thiene G, Yilmaz A, Charron P, Elliott PM. Current state of knowledge on aetiology, diagnosis, management, and therapy of myocarditis: a position statement of the European Society of Cardiology working group on myocardial and pericardial diseases. *Eur Heart J* 2013; **34**: 2636–2648 2648a–2648d.
- Frustaci A, Russo MA, Chimenti C. Randomized study on the efficacy of immunosuppressive therapy in patients with virus-negative inflammatory cardiomyopathy: the TIMIC study. *Eur Heart J* 2009; **30**: 1995–2002.
- Leone O, Veinot JP, Angelini A, Baandrup UT, Basso C, Berry G, Bruneval P, Burke M, Butany J, Calabrese F, d'Amati G, Edwards WD, Fallon JT, Fishbein MC, Gallagher PJ, Halushka MK, McManus B, Pucci A, Rodriguez ER, Saffitz JE, Sheppard MN, Steenbergen C, Stone JR, Tan C, Thiene G, van der Wal AC, Winters GL. 2011 consensus statement on endomyocardial biopsy from the Association for European Cardiovascular Pathology and the Society for Cardiovascular Pathology. *Cardiovasc Pathol* 2012; **21**: 245–274.
- Holzmann M, Nicko A, Kühl U, Noutsias M, Poller W, Hoffmann W, Morguet A, Witzensbichler B, Tschöpe C, Schultheiss H-P, Pauschinger M. Complication rate of right ventricular endomyocardial biopsy via the femoral approach: a retrospective and prospective study analyzing 3048 diagnostic procedures over an 11-year period. *Circulation* 2008; **118**: 1722–1728.
- Yilmaz A, Kindermann I, Kindermann M, Mahfoud F, Ukena C, Athanasiadis A, Hill S, Mahrholdt H, Voehringer M, Schieber M, Klingel K, Kandolf R, Böhm M, Sechtem U. Comparative evaluation of left and right ventricular endomyocardial biopsy: differences in complication rate and diagnostic performance. *Circulation* 2010; **122**: 900–909.
- Ferreira VM, Piechnik SK, Dall'Armellina E, Karamitsos TD, Francis JM, Ntusi N, Holloway C, Choudhury RP, Kardos A, Robson MD, Friedrich MG, Neubauer S. T(1) mapping for the diagnosis of acute myocarditis using CMR: comparison to T2-weighted and late gadolinium

- enhanced imaging. *JACC Cardiovasc Imaging* 2013; **6**: 1048–1058.
14. Lota AS, Gatehouse PD, Mohiaddin RH. T2 mapping and T2* imaging in heart failure. *Heart Fail Rev* 2017; **22**: 431–440.
 15. Taylor AJ, Salerno M, Dharmakumar R, Jerosch-Herold M. T1 mapping: basic techniques and clinical applications. *JACC Cardiovasc Imaging* 2016; **9**: 67–81.
 16. Moon JC, Messroghli DR, Kellman P, Piechnik SK, Robson MD, Ugander M, Gatehouse PD, Arai AE, Friedrich MG, Neubauer S, Schulz-Menger J, Schelbert EB. Myocardial T1 mapping and extracellular volume quantification: a Society for Cardiovascular Magnetic Resonance (SCMR) and CMR working group of the European Society of Cardiology consensus statement. *J Cardiovasc Magn Reson* 2013; **15**: 92.
 17. Spieker M, Katsianos E, Gastl M, Behm P, Horn P, Jacoby C, Schnackenburg B, Reinecke P, Kelm M, Westenfeld R, Böner F. T2 mapping cardiovascular magnetic resonance identifies the presence of myocardial inflammation in patients with dilated cardiomyopathy as compared to endomyocardial biopsy. *Eur Heart J Cardiovasc Imaging* 2018; **19**: 574–582.
 18. Cooper LT, Baughman KL, Feldman AM, Frustaci A, Jessup M, Kuhl U, Levine GN, Narula J, Starling RC, Towbin J, Virmani R. The role of endomyocardial biopsy in the management of cardiovascular disease: a scientific statement from the American Heart Association, the American College of Cardiology, and the European Society of Cardiology endorsed by the Heart Failure Society of America and the Heart Failure Association of the European Society of Cardiology. *Eur Heart J* 2007; **28**: 3076–3093.
 19. Cerqueira MD, Weissman NJ, Dilsizian V, Jacobs AK, Kaul S, Laskey WK, Pennell DJ, Rumberger JA, Ryan T, Verani MS. Standardized myocardial segmentation and nomenclature for tomographic imaging of the heart. A statement for healthcare professionals from the Cardiac Imaging Committee of the Council on Clinical Cardiology of the American Heart Association. *Circulation* 2002; **105**: 539–542.
 20. Schulz E, Jabs A, Gori T, Hink U, Sotiriou E, Tschöpe C, Schultheiss H-P, Münzel T, Wenzel P. Feasibility and safety of left ventricular endomyocardial biopsy via transradial access: technique and initial experience. *Catheter Cardiovasc Interv* 2015; **86**: 761–765.
 21. Escher F, Kühl U, Lassner D, Stroux A, Westermann D, Skurk C, Tschöpe C, Poller W, Schultheiss H-P. Presence of perforin in endomyocardial biopsies of patients with inflammatory cardiomyopathy predicts poor outcome. *Eur J Heart Fail* 2014; **16**: 1066–1072.
 22. Badorff C, Noutsias M, Kühl U, Schultheiss H-P. Cell-mediated cytotoxicity in hearts with dilated cardiomyopathy: correlation with interstitial fibrosis and foci of activated T lymphocytes. *J Am Coll Cardiol* 1997; **29**: 429–434.
 23. Noutsias M, Pauschinger M, Ostermann K, Escher F, Blohm J-H, Schultheiss H, Kühl U. Digital image analysis system for the quantification of infiltrates and cell adhesion molecules in inflammatory cardiomyopathy. *Med Sci Monit* 2002; **8**: MT59–MT71.
 24. R Core Team. R: a language and environment for statistical computing. Vienna, Austria; 2019. <https://www.R-project.org/> Accessed November 30, 2019.
 25. Baeßler B, Schaarschmidt F, Dick A, Stehning C, Schnackenburg B, Michels G, Maintz D, Bunck AC. Mapping tissue inhomogeneity in acute myocarditis: a novel analytical approach to quantitative myocardial edema imaging by T2-mapping. *J Cardiovasc Magn Reson* 2015; **17**: 115.
 26. Nishii T, Kono AK, Shigeru M, Takamine S, Fujiwara S, Kyotani K, Aoyama N, Sugimura K. Cardiovascular magnetic resonance T2 mapping can detect myocardial edema in idiopathic dilated cardiomyopathy. *Int J Cardiovasc Imaging* 2014; **30**: 65–72.
 27. Minegishi S, Kato S, Takase-Minegishi K, Horita N, Azushima K, Wakui H, Ishigami T, Kosuge M, Kimura K, Tamura K. Native T1 time and extracellular volume fraction in differentiation of normal myocardium from non-ischemic dilated and hypertrophic cardiomyopathy myocardium: a systematic review and meta-analysis. *Int J Cardiol Heart Vasc* 2019; **25**: 100422.
 28. Baessler B, Luecke C, Lurz J, Klingel K, Das A, von Roeder M, de Waha-Thiele S, Besler C, Rommel KP, Maintz D, Gutberlet M. Cardiac MRI and texture analysis of myocardial T1 and T2 maps in myocarditis with acute versus chronic symptoms of heart failure. *Radiology* 2019; **292**: 608–617.
 29. Lurz P, Eitel I, Adam J, Steiner J, Grothoff M, Desch S, Fuernau G, de Waha S, Sareban M, Luecke C, Klingel K, Kandolf R, Schuler G, Gutberlet M, Thiele H. Diagnostic performance of CMR imaging compared with EMB in patients with suspected myocarditis. *JACC Cardiovasc Imaging* 2012; **5**: 513–524.
 30. Kellman P, Hansen MS. T1-mapping in the heart: accuracy and precision. *J Cardiovasc Magn Reson* 2014; **16**: 2.
 31. Kim PK, Hong YJ, Im DJ, Suh YJ, Park CH, Kim JY, Chang S, Lee H-J, Hur J, Kim YJ, Choi BW. Myocardial T1 and T2 mapping: techniques and clinical applications. *Korean J Radiol* 2017; **18**: 113–131.
 32. Lurz P, Luecke C, Eitel I, Föhrenbach F, Frank C, Grothoff M, de Waha S, Rommel K-P, Lurz JA, Klingel K, Kandolf R, Schuler G, Thiele H, Gutberlet M. Comprehensive cardiac magnetic resonance imaging in patients with suspected myocarditis: The MyoRacer-trial. *J Am Coll Cardiol* 2016; **67**: 1800–1811.
 33. Müller A, Jurcoane A, Kebir S, Ditter P, Schrader F, Herrlinger U, Tzaridis T, Mädler B, Schild HH, Glas M, Hattingen E. Quantitative T1-mapping detects cloudy-enhancing tumor compartments predicting outcome of patients with glioblastoma. *Cancer Med* 2017; **6**: 89–99.
 34. Xu X, Zhang H-L, Liu Q-P, Sun S-W, Zhang J, Zhu F-P, Yang G, Yan X, Zhang Y-D, Liu X-S. Radiomic analysis of contrast-enhanced CT predicts microvascular invasion and outcome in hepatocellular carcinoma. *J Hepatol* 2019; **70**: 1133–1144.
 35. Liu Z, Wang S, Di Dong WJ, Fang C, Zhou X, Sun K, Li L, Li B, Wang M, Tian J. The applications of radiomics in precision diagnosis and treatment of oncology: opportunities and challenges. *Theranostics* 2019; **9**: 1303–1322.
 36. Sotiriou E, Heiner S, Jansen T, Brandt M, Schmidt KH, Kreitner K-F, Emrich T, Schultheiss H-P, Schulz E, Münzel T, Wenzel P. Therapeutic implications of a combined diagnostic workup including endomyocardial biopsy in an all-comer population of patients with heart failure: a retrospective analysis. *ESC Heart Fail* 2018; **5**: 630–641.
 37. Frey N, Meder B, Katus HA. Left ventricular biopsy in the diagnosis of myocardial diseases. *Circulation* 2018; **137**: 993–995.